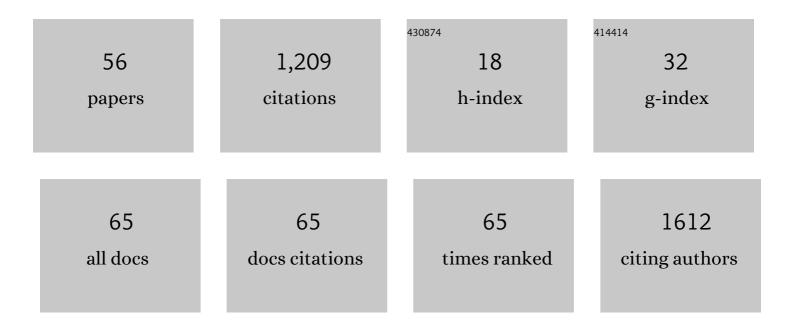
Leonel Malacrida

List of Publications by Year in descending order

Source: https://exaly.com/author-pdf/600088/publications.pdf Version: 2024-02-01



#	Article	IF	CITATIONS
1	Fit-free analysis of fluorescence lifetime imaging data using the phasor approach. Nature Protocols, 2018, 13, 1979-2004.	12.0	217
2	PTEN Deficiency and AMPK Activation Promote Nutrient Scavenging and Anabolism in Prostate Cancer Cells. Cancer Discovery, 2018, 8, 866-883.	9.4	141
3	Measurements of absolute concentrations of NADH in cells using the phasor FLIM method. Biomedical Optics Express, 2016, 7, 2441.	2.9	88
4	The Phasor Plot: A Universal Circle to Advance Fluorescence Lifetime Analysis and Interpretation. Annual Review of Biophysics, 2021, 50, 575-593.	10.0	67
5	Spectral phasor analysis of LAURDAN fluorescence in live A549 lung cells to study the hydration and time evolution of intracellular lamellar body-like structures. Biochimica Et Biophysica Acta - Biomembranes, 2016, 1858, 2625-2635.	2.6	62
6	LAURDAN since Weber: The Quest for Visualizing Membrane Heterogeneity. Accounts of Chemical Research, 2021, 54, 976-987.	15.6	50
7	A multidimensional phasor approach reveals LAURDAN photophysics in NIH-3T3 cell membranes. Scientific Reports, 2017, 7, 9215.	3.3	47
8	Model-free methods to study membrane environmental probes: a comparison of the spectral phasor and generalized polarization approaches. Methods and Applications in Fluorescence, 2015, 3, 047001.	2.3	41
9	Alteration in Fluidity of Cell Plasma Membrane in Huntington Disease Revealed by Spectral Phasor Analysis. Scientific Reports, 2018, 8, 734.	3.3	41
10	Determination of the metabolic index using the fluorescence lifetime of free and bound nicotinamide adenine dinucleotide using the phasor approach. Journal of Biophotonics, 2019, 12, e201900156.	2.3	41
11	A global view of standards for open image data formats and repositories. Nature Methods, 2021, 18, 1440-1446.	19.0	36
12	LAURDAN fluorescence and phasor plots reveal the effects of a H2O2 bolus in NIH-3T3 fibroblast membranes dynamics and hydration. Free Radical Biology and Medicine, 2018, 128, 144-156.	2.9	33
13	Phasor-based hyperspectral snapshot microscopy allows fast imaging of live, three-dimensional tissues for biomedical applications. Communications Biology, 2021, 4, 721.	4.4	30
14	Delayed mTOR Inhibition with Low Dose of Everolimus Reduces TGFβ Expression, Attenuates Proteinuria and Renal Damage in the Renal Mass Reduction Model. PLoS ONE, 2012, 7, e32516.	2.5	30
15	Visualization of barriers and obstacles to molecular diffusion in live cells by spatial pair-cross-correlation in two dimensions. Biomedical Optics Express, 2018, 9, 303.	2.9	26
16	Hyperoxia and Lungs: What We Have Learned From Animal Models. Frontiers in Medicine, 2021, 8, 606678.	2.6	26
17	StarD5: an ER stress protein regulates plasma membrane and intracellular cholesterol homeostasis. Journal of Lipid Research, 2019, 60, 1087-1098.	4.2	25
18	sideSPIM – selective plane illumination based on a conventional inverted microscope. Biomedical Optics Express, 2017, 8, 3918.	2.9	22

LEONEL MALACRIDA

#	Article	IF	CITATIONS
19	The DIVER Microscope for Imaging in Scattering Media. Methods and Protocols, 2019, 2, 53.	2.0	22
20	Differences between FLIM phasor analyses for data collected with the Becker and Hickl SPC830 card and with the FLIMbox card. Microscopy Research and Technique, 2018, 81, 980-989.	2.2	19
21	Spectral phasor analysis reveals altered membrane order and function of root hair cells in Arabidopsis dry2/sqe1-5 drought hypersensitive mutant. Plant Physiology and Biochemistry, 2017, 119, 224-231.	5.8	18
22	CAPRYDAA, an anthracene dye analog to LAURDAN: a comparative study using cuvette and microscopy. Journal of Materials Chemistry B, 2020, 8, 88-99.	5.8	18
23	Linear Combination Properties of the Phasor Space in Fluorescence Imaging. Sensors, 2022, 22, 999.	3.8	16
24	Comparison between iMSD and 2D-pCF analysis for molecular motion studies on in vivo cells: The case of the epidermal growth factor receptor. Methods, 2018, 140-141, 74-84.	3.8	12
25	In vivo macromolecular crowding is differentially modulated by aquaporin 0 in zebrafish lens: Insights from a nanoenvironment sensor and spectral imaging. Science Advances, 2022, 8, eabj4833.	10.3	11
26	Adenosine triphosphate–dependent calcium signaling during ventilator-induced lung injury is amplified by hypercapnia. Experimental Lung Research, 2011, 37, 471-481.	1.2	9
27	Sevoflurane anesthesia deteriorates pulmonary surfactant promoting alveolar collapse in male Sprague–Dawley rats. Pulmonary Pharmacology and Therapeutics, 2014, 28, 122-129.	2.6	9
28	A novel nitroalkeneâ€Î±â€ŧocopherol analogue inhibits inflammation and ameliorates atherosclerosis in Apo E knockout mice. British Journal of Pharmacology, 2019, 176, 757-772.	5.4	9
29	Membrane Remodeling by Arc/Arg3.1. Frontiers in Molecular Biosciences, 2021, 8, 630625.	3.5	8
30	Redox Behavior of Re(V)–Amino Acid Containing Complexes. Journal of Colloid and Interface Science, 2002, 249, 366-371.	9.4	6
31	Fluorescence Lifetime Phasor Analysis of the Decamer–Dimer Equilibrium of Human Peroxiredoxin 1. International Journal of Molecular Sciences, 2022, 23, 5260.	4.1	5
32	Insights into <i>in vivo</i> adipocyte differentiation through cell-specific labeling in zebrafish. Biology Open, 2021, 10, .	1.2	4
33	Salbutamol Improves Diaphragmatic Contractility in Chronic Airway Obstruction. Archivos De Bronconeumologia, 2009, 45, 230-234.	0.8	3
34	Halogenated Anesthetics Impairs Biophysical Properties of a Membrane Model of Pulmonary Surfactant. Biophysical Journal, 2011, 100, 505a-506a.	0.5	3
35	Barriers to Diffusion in Cells: Visualization of Membraneless Particles in the Nucleus. The Biophysicist, 2020, 1, .	0.3	2
36	Halogenated Anesthetics Impairs Phospholipid Composition From A Pulmonary Surfactant System. , 2010, , .		0

LEONEL MALACRIDA

#	Article	IF	CITATIONS
37	Halogenated Anesthetics Impairs Biophysical Properties Of Pulmonary Surfactant. , 2011, , .		Ο
38	Deterioration of Pulmonary Surfactant by Volatile Anesthetics. Biophysical Journal, 2012, 102, 496a.	0.5	0
39	Sleeping Bubbles: Effects of Volatile Anesthetics in the Lateral Structure of Giant Unilamellar Vesicles. Biophysical Journal, 2013, 104, 33a.	0.5	Ο
40	Phasor Plots and Spectral Phasor Analysis of Laurdan and Prodan for Membrane Heterogeneity Studies: New Frontiers in Membrane Biophysics. Biophysical Journal, 2014, 106, 84a.	0.5	0
41	Hydration and Supramolecular Organization Studies of Lamellar Bodies in A549 Lung Cells using Laurdan Fluorescence. Biophysical Journal, 2015, 108, 413a.	0.5	Ο
42	Linear Combination between Lifetime and Spectral Phasor Plots: A New Approach to Study Membrane Organization with Laurdan. Biophysical Journal, 2016, 110, 492a.	0.5	0
43	Water Activity Inside the Nucleus: Some Clues using ACDAN Fluorescence and its Implications in the Chromatin Supramolecular Organization. Biophysical Journal, 2017, 112, 218a.	0.5	0
44	Of Absolute Concentrations of NADH in Cells using the Phasor Flim Method. Biophysical Journal, 2017, 112, 581a.	0.5	0
45	Selective Plane Illumination Microscopy in the Conventional Inverted Microscope Geometry. Biophysical Journal, 2017, 112, 145a.	0.5	0
46	SideSPIM - A Flexible Multipurpose Platform for Light Sheet Microscopy. Biophysical Journal, 2018, 114, 187a.	0.5	0
47	Elucidating Invisible Barriers and Obstacles to Molecular Diffusion in Live Cells by the Spatial Pair-Correlation Function: A Connectivity View of the Cell. Biophysical Journal, 2018, 114, 166a.	0.5	0
48	Intracellular Transport Characterization of the Transcription Factor Gli2 by Fluorescence Correlation Spectroscopy Approaches. Biophysical Journal, 2018, 114, 630a.	0.5	0
49	Photophysical Characterization and Microscopy Application of an Anthracene Analogous of Laurdan. Biophysical Journal, 2019, 116, 81a.	0.5	0
50	The Fluorescence Lifetime of Bound NADH: Clues from the Phasor Plots. Biophysical Journal, 2019, 116, 565a.	0.5	0
51	In Vivo Chromatin Compaction Changes as Detected by Water Dipolar Relaxations: the Molecular Crowding Role Revealed by the Acdan Fluorescence. Biophysical Journal, 2019, 116, 70a.	0.5	0
52	Characterization of the Metabolic State and Molecular Crowding in Breast Cancer Spheroids. Biophysical Journal, 2019, 116, 421a.	0.5	0
53	Multi-Modal Fluorescence Characterization of Cell Cycle Progression and Cytokinesis. Biophysical Journal, 2019, 116, 24a.	0.5	0
54	Primary Cilium Submicron Organization and Dynamics. Biophysical Journal, 2020, 118, 437a.	0.5	0

#	Article	IF	CITATIONS
55	Measuring the Spatial Distribution of Dipolar Relaxation in Live Zebrafish Eye Lenses during Development. Biophysical Journal, 2020, 118, 308a.	0.5	0
56	Solvatochromic Properties of Acdan and Spectral Phasor Analysis Reveal the Role of Aquaporin OA in Regulating Macromolecular Crowding in the Zebrafish Lens In Vivo. Biophysical Journal, 2020, 118, 166a.	0.5	0